Proceedings Paper:
Liu, X, Liu, Q, Wu, Z et al. (2019) Mixed-Model Noise Removal in 3D MRI via Rotation-and-Scale Invariant Non-Local Means. In: Lecture Notes in Computer Science. SaMBa 2018: Processing and Analysis of Biomedical Information., 20 Sep 2018, Granada, Spain. Springer Verlag, pp. 33-41. ISBN: 9783030138349. ISSN: 0302-9743. EISSN: 1611-3349.

https://doi.org/10.1007/978-3-030-13835-6_5

Mixed-model Noise Removal in 3D MRI via Rotation-and-Scale Invariant Non-Local Means

No Author Given

No Institute Given

Abstract. Mixed noise is a major issue influencing quantitative analysis in different forms of magnetic resonance image (MRI), such as T1 and diffusion image like DWI and DTI. Using different filters sequentially to remove mixed noise will severely deteriorate such medical images. We present a novel algorithm called rotation-and-scale invariant nonlocal means filter (RSNLM) to simultaneously remove mixed noise from different kinds of three-dimensional (3D) MRI scan. Firstly, new similarity weights including rank-ordered absolute difference (ROAD) with a trilateral filter (TriF) are obtained to detect the mixed and high level noise. Then, we present a geometric view to consider the MRI data as 3D operator, with which the similarity between the patches is calculated canceling the relative rigid transformation, so that translation, rotation and scaling transformation have no influence on the similarity. Lastly, we illustrate an adaptive parameter estimation method for ROAD. We present a mathematical proof of the validity of the algorithm. We also evaluate the algorithm capabilities with several experiments using synthetic data with impulse noise, Rician noise and real MRI data. The results confirm that our method has superior performance overcoming the state-of-the-art methods.

1 Introduction

With Modern MRI reconstruction systems, the resulting noise is more complicated than the traditional Rician distribution with constant noise power [1], involving mixed types of noise. During the transmission, impulse noise will also be generated in MRIs via noisy sensors, communication channels, transmission apparatus, etc. Simultaneously removing all these noise types keeping the meaningful edges is a critical problem for the medical image processing.

Previous works have focused on removing the traditional MRI noise model, rician noise, with the non-local means(NLM) [2] method, which has particularly good performance in edge-preserving. Coupé et al [5] introduced NLM in MRI denoising, and then Wiest used it on diffusion MRI dataset [12]. The key features of NLM are that it uses non-local information and self-similarity weights for denoising. Recently, Manjón [9] proposed method of prefiltered rotationally invariant NLM3D(Pri-NLM) with combining different filter together. Chen et al [3] calculated the neighborhood both on the spatial and wavevector space in a series of papers to obtain the good result. However, few paper discussed mixed noise removal and different kinds of weight design.

There are two main approaches to removing the mixture of Rician noise and impulse noise from MRI: removing different kinds of noise in multiple steps or simultaneously. For the first approach, one common method is to combine a Rician filter and an impulse filter together. The proposed BM4DM is a filter that integrate the BM4D [8] and median filters, and was adopted to remove two models noise respectively. However, the intensity of pixels is often changed by the first filter, in that they usually invalidate efforts to remove the other noise in subsequent steps, and vice versa. For the second approach, Garnett [11] introduced the ROAD statistic for the detection of pixels contaminated by impulse noise, and integrated it into the bilateral filter to construct the trilateral filter (TriF [7]). The patch-based weighted means filter [6] improved the TriF with the weights extended from NLM.

In this paper, we adopt the second approach and present a new method, RSNLM, to remove the mixed noise simultaneously from the 3D MRI data. Our main contributions are threefold: (1) We combine the ideas of NLM and TriF to remove the mixed noise simultaneously for the high self-similarity of 3D MRI data. (2) We consider the 3D patch as a 3D volume shape model in a computer graphics view. We eliminate the rigid transformation (translation, rotation and scaling) to calculate the similarity of different 3D patches. (3) We propose a automatic parameter selection of the ROAD statistic, making the algorithm adaptive and efficient for detecting and removing high level impulse noises

2 Methods

Problem formulation. Various noises will coexist in MR images, especially Rician noise and impulse noise. Due to the distribution of impulsive noise, the pixel destroyed by impulse noise is always clearly different from its surrounding pixels. The noise level of impulse noise is defined by p, which is the probability that a given pixel is corrupted by impulse noise. It is known that the magnitude of an MR image is computed from the real image and imaginary image, both containing Gaussian distributed noise. Thus, the noise contained in the magnitude MRI follows a Rician distribution [10]. The main concept behind NLM is to estimate each pixel by a weighted mean of the observed values $v(j)$, for j in search window, $N_i(D)$, and with weights depending on the similarity between local patches centered at i and j. More precisely, the NLM filter is defined as

$$\hat{v}\,(i) = \frac{\sum_{j\in N_i(D)} w(i,j)v(j)}{\sum_{j\in N_i(D)} w(i,j)}, \quad \text{with} \quad w(i,j) = e^{-\|v(N_i)-v(N_j)\|_2^2/(2\sigma_h^2)}, \qquad (1)$$

where N_i is a 3D patch of d^3 pixels centered at i, and $v(N_i)$ is the vector composed of those pixels, arranged in a fixed order. The similarity between two patches is measured by the L_2-distance, $\|v(N_i) - v(N_j)\|_2$. The classic NLM is designed to remove Gaussian noise. We propose a modification based on [5] for the unbiased removal of the noncentral Rician distributed noise:

$$\hat{v}\,(i) = \sqrt{\max\left(\left(\frac{\sum_{j\in N_i(D)} w(i,j)v^2(j)}{\sum_{j\in N_i(D)} w(i,j)}\right) - 2\sigma^2, 0\right)} \qquad (2)$$

σ is the noise level. Our study focuses on finding an effective strategy for describing the similarity of patches and then calculating better weights. An overview of our method is summarized in Alg.1.

Algorithm 1 The RSNLM Algorithm

Require:
Noisy MRI data: I;
The set of hyper-parameter: $\Theta = \{D, d, \sigma_I, \sigma_M, \sigma_S, \sigma_{SM}\}$;
Ensure:
Estimate parameter m in ROAD statistic ;
A D^3 search window ;
A d^3 similar patch;
repeat
  Moving the search window $N_i(D)$ centered at $i \in I$;
  Get the estimative patch $N_i(d)$ centered at i ;
  repeat
    Moving the similar patch $N_j(d)$ centered at $j \in N_i(D)$;
    Find $N_i(d)$'s most similar patch by the rigid transformation of $N_j(d)$.
    Calculate $w(i,j)$ by Eq.3;
  until Traverse all the points in $N_i(D)$.
  Obtain the estimation intensity result of pixel i,$O(i)=\hat{v}(i)$
until Traverse all the points in I.
return The restored MRI data O.

Weights estimation in RSNLM The patch similarity of RSNLM defined in Eq. 3.

$$w(i,j)=w_s(i,j)w_I(i,j)w_{MR}(i,j) \tag{3}$$

Inspired by TriF, we utilize ROAD [11] to detect pixels contaminated by impulse noise and other high level noise. We consider three factors to express the similarity between patches i and j and their weight $w(i,j)$. By theory, in fact, a local similarity is more reliable than a farther away one. In that, the spatial weight is defined as $w_s(i,j) = e^{-\|i-j\|_2^2/(2\sigma_S^2)}$, where $\|i-j\|$ is the spatial distance between pixel i and j.

The impulse detective weight is defined as $w_I(i,j) = e^{-ROAD(j)^2/(2\sigma_I^2)}$, which is close to zero if j is an impulse noisy point or serious different from its surrounding pixels. The value of $ROAD$ at pixel j is defined as $ROAD(j)=\sum_{k=1}^{m} r_k(j)$ where $r_k(j)$ is the k-th term in the set $\{|v(i)-v(j)| : i \in N_j(R) \setminus \{j\}\}$ arranged in an ascending order with some terms possibly equal. If j is a impulse noise or in patch j where impulse noise exists, then $ROAD(j)$ will be very high. The similar weight w_{MR} describes the similarity of pixel values between two patches as

$$w_{MR}(i,j) = e^{-(\|v(N_i)-v(N_j)\|_{SR})^2/(2\sigma_{MR}^2)} \tag{4}$$

$$\text{where} \quad \|v(N_i) - v(N_j)\|_{SR} = \inf_{\substack{r\in[0,2\pi] \\ t\in[1,2]}} \|v(N_i) - v(S_t R_r N_j)\|$$

$$= \sqrt{\frac{\sum_{k\in N_0} w_s(j,k) J_I(i+k, j+S_t R_r k) \left|v(i+k) - v(j+S_t R_r k)\right|^2}{\sum_{k\in N_0} w_s(j,k) J_I(i+k, j+S_t R_r k)}}.$$

$S_t R_r$ represents the rotation angle of r and shrinking t times with respect to the origin 0. $S_t R_r N_j$ stands for the rotation and scaling of N_j with respect to its center j, i.e, $S_t R_r N_j = \left\{j + S_t R_r k : k \in N_j^0\right\}$, N_j^0 is the most primitive patch centered at j without rigid transformation of N_j. The above defined $w_s(j,k)$ is used to describe the spatial distance between j and k, giving more importance to similarity between closer pixels. The term $J_I(i+k, j+S_t R_r k)$, as the joint impulse coefficient of $i+k$ and $j+S_t R_r k$, is defined as $J_I(i+k, j+S_t R_r k) = w_I(i+k) w_I(j+S_t R_r k)$, and is used to remove the influence of impulse noise pixels in the similarity measure.

With these three weights, we can detect the impulse noise and high level other noise and simultaneously remove all kinds of noise.

Ridge transformation of the compared patch. From shape view, the ridge transformation(translation, scaling, and rotation) of the patch should have no influence on the similarity between patches, $\|v(N_i) - v(N_j)\|_{SR}$ in Eq.4.

Translation invariance. With patch movement, the original location of the patch in the window has no influence on similarity. **Scale invariance.** In our method, we obtain smaller copies of the original images by taking a morphological transformation, where t is the reduced ratio. The patch size d of j is $(2^3)^{t-1}$ bigger than the patch i. With interlacing downsampling $t-1$ times, we can eliminate the influence on multi-scale and obtain more compared patch. **Rotation invariance.** To complete rotation in 3D space, we decomposed the process into three 2D rotations around the three axes (x, y, z) respectively shown in Fig. 2. A window can be divided into eight parts (①∼⑧), with which the pose of the patch can be determined by finding one part's position after the rotation. To minimize $\|v(N_i) - v(N_j)\|_{SR}$ on $r \in [0, 2\pi]$, we used the discrete solution of minimizing over the set of a finite number of angles, for $r \in \{2\pi k/n, k = 0, 1, \cdots, n-1\}$ with $n > 1$ as a suitable integer. n is set as a function of the size of cubes $N_i(d)$; in our experiments we choose $n = 4(d-1)$. Set $n = 16$ for $d \geq 5$ for the time complexity.

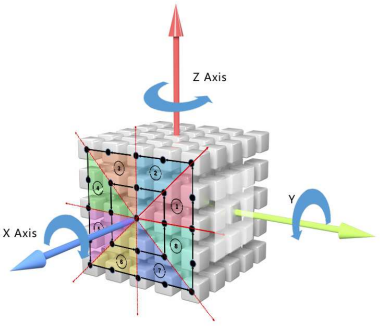

Fig. 1: Rotation diagram

Adaptive ROAD parameter. The parameter m in ROAD is an important factor for detecting the impulse level which should not be constant as [11]. We

set m as a function of the impulse noisy level p. X, the number of non-impulse noisy points in $N_i(R)$, follows binomial distribution with parameters $R \times R \times R$ and $1-p$. The probability of $X{=}k$ is $P(X=k){=}C^k_{R\times R\times R}(1-p)^k p^{R\times R\times R-k}$. The choice of m should ensure that $X{=}k$ with great probability, that $P(X \geq m) \geq p_c$, with p_c close to 1, called the confidence probability. Therefore, we choose m as the largest integer in $\sum_{k=m}^{R\times R\times R} P(X=k) \geq p_c$. For example, in our experiments we set $p_c = 0.95$. Therefore, as examples, for $R{=}3$ we have $m = 14$ if $p = 0.1$.

Proof of algorithm validity The effectiveness and unbiasedness of $\hat{v}\,(i)$ is considered to prove the validity of our algorithm. According to the *Law of Large Numbers*, we can draw the expectation of $\hat{v}^2(i) - u^2(i)$ as $E_i{=}E(\hat{v}^2(i) - u^2(i)) = \sum_j \frac{w_j}{w}(u^2(j) - u^2(i))$, with the number of noisy pixels n increasing unlimited, The E_i will be small when $x_1 \leq x_2 \leq \cdots \leq x_t$ and $w_t \leq w_{t-1} \leq \cdots \leq w_1$, where x_j is the absolute value of $u^2(j) - u^2(i)$. Actually, changing on these two orders would trigger the increase of E_i. To maintain these orders, it is necessary to find a strategy that can describe the similarity of $u(i)$ and $u(j)$ well. Besides that, we also consider the $D(\hat{v}^2(i))$, the unbiasedness of $\hat{v}^2(i)$, that can be written as $D(\hat{v}^2(i)){=}\sum_j \frac{w_j^2}{w^2}\sigma^2$. According to the *Cauchy inequality*, we obtain the minimum of $D(\hat{v}^2(i))$ if and only if $w_1{=}w_2{=}w_3{=}\cdots{=}w_m{=}\frac{1}{m}$, where m is the number of w_j that satisfies $w_j \neq 0$. $D(\hat{v}^2(i))$ is an increasing function of the difference between w_k and w_l,with $\forall k, l \in N_i(D)$. The above analysis and proof motivates us to find the most similar patches even with the accidental effect caused by noise interference. The larger the cubes are, the smaller the similar contingency is, which makes results more credible. Based on contextual analysis, we provide the rotationally and scaling invariant similarity measure to find more similar patches and then obtain the best estimation of $u(i)$.

3 Experiments and Discussion

In this section, we report several experiments that we conducted to compare the RSNLM with BM4DM, TriF, and Pri-NLM using a platform constructed in MATLAB 2015b and Visual Studio 2012. To measure the quality of the l-ter, PSNR and SSIM are adopted to measure the quality of restored images. Our experiments are done on both synthetic data and clinical data respectively. The synthetic MRIs (T1) with 1 mm^3 voxel resolution (8 bit quantization) were from BrainWeb [4] and had different noise models (Rician, impulse) at different level. The clinical data (DWI and DTI with 2.5mm isotropic resolution) were downloaded from In Vivo Human Database acquired under Human Brain Project and National Research Resource Center grant.

Synthetic data. The denoising results of one T1 weighted image and it's regional close-up views of each methods are shown in Fig.2. The results demonstrate the remarkable noise removing and edge-preserving property of RSNLM. In the case of noise level (0.1,3), we set $\Theta{=}\{7, 3, 358, 42, 0.4, 2\}$. In Fig.2, we

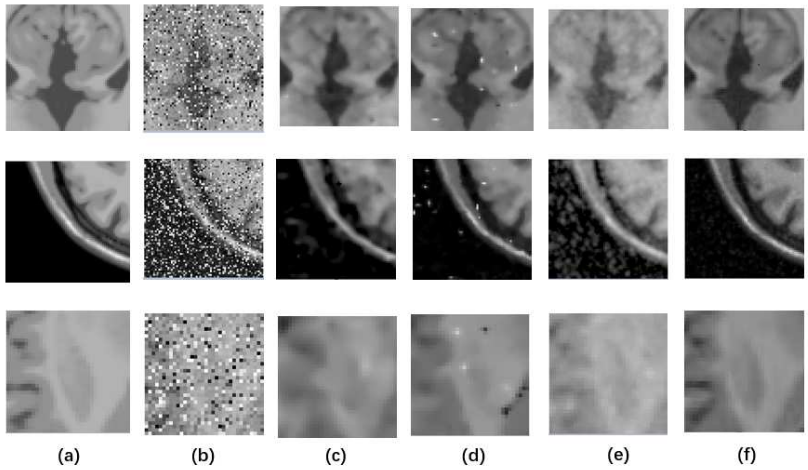

Fig. 2. Filtering results of an axial slice of T1 weighted Brain Web (Rician noise level of 5% and impulse noise level of p=0.3). These three rows of images correspond to the results of three local parts respectively. Each column corresponds to (a)original image, (b)noisy image, result from (c)TriF, (d)Pri-NLM, (e)BM4DM and (f)RSNLM.

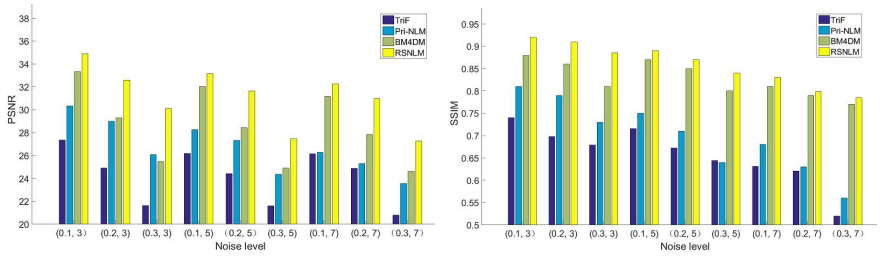

(a) PSNR (b) SSIM

Fig. 3. The average results of PSNR (a) and SSIM (b) of five T1 weighted images with different noise level. '(A,B)' express the noise level with 'A' for impulse noise and 'B' for Rician noise on horizontal axis. From left to right color (purple:TriF, blue:Pri-NLM, green: BM4DM and yellow: RSNLM) represent different methods with histograms.

can see the detail and texture of the cerebral cortex(line 2) and white matter(line 3) keeps better by our RSNLM than the other method. As observed in Fig.2(c)(d)'s, TriF and Pri-NLM removed most of the noise but still remain impulse noise and blurred the image. BM4DM(in Fig.2(e)) perform better than other two methods, but still worse than RSNLM in preserving the boundary. Fig. 3 shows the average of 5 sets of synthetic T1 weighted images denoising results(PSNR, SSIM). Though the denoising result indicates that our method, RSNLM, performance better than other compared methods in PSNR and SSIM values with different noise levels. Our method provide the best PSNR 34.9 with

SSIM 92.3% on $p = 0.1$ and $\sigma = 3$. Compared with the second best method BM4DM, the average improvement with 2.59 in PSNR and 3% in SSIM. That means the high level mixed noise can be satisfactorily removed by RSNLM with the edge preservation.

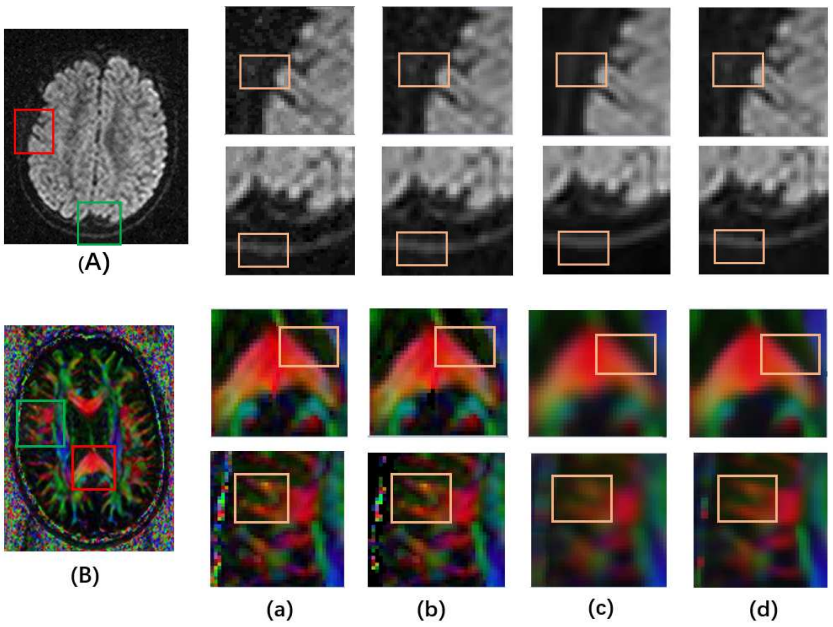

Fig. 4. Filtering results of an axial slice of DWI. The left parts of this figure is the original DWI (A) and DTI(B) slice and it's two local fields (red and blue) to be enlarged shown on the right. it's closed-up views. These first and second rows on the right part of this figure are respectively the closed-up view of red and blue filed with different filtering methods (a)TriF, (b)Pri-NLM, (c)BM4DM and (d)RSNLM.

Clinical data. We verify our method with clinical diffusion data(DWI and DTI) in Fig. 4. Compared with the experiments on synthetic data, the D-Otsu (combine *distance constraints* and classic Otsu) is provided to segment the diffusion MRI as foreground and the background used to estimate the noise level σ. The proportion of abnormal points in background is taken as the value of p. When performing DTI filtering, we consider the similarity of eigenvectors and eigenvalues of diffusion matrix rather than the similarity based on pixels. The hyper-parameter set Θ is assigned as $\Theta = \{7, 3, 375, 13.5, 0.5, 4.5\}$ in DTI image. In case of filtering DWI, the value of estimated σ and p are respectively 27.5 and 0.093, with $\Theta = \{5, 3, 610, 21, 0.6, 2\}$. Just as shown in Fig. 4, in the tensor field, the BM4DM and RSNLM are also confirmed to be effective in preserving edges while removing noise. But the TriF and Pri-NLM blur structural boundaries

especially on the orange rectangle in enlarged parts. With similar result comes from the Fractional Anisotropy (FA) of DTI with four methods. The RSNLM reduces the ambiguity and unevenness of FA boundaries caused by noise than BM4DM.

4 Conclusion

We provide a novel filter for 3D MRI mixed noise removing simultaneously via rotation-and scale invariant nonlocal means filter. We combine the shape view with statistic view together to treat the mixed noise of MRI image. Our method over performance state-of-the-art method as TriF, Pri-NLM and BM4DM not only with recover visualization but also with data analysis in PSNR and SSIM. In future we would like to extend our method to other medical image denoising problem and models.

References

1. S. Aja-Fernández and G. Vegas-Sánchez-Ferrero. Statistical noise models for MRI. In *Statistical Analysis of Noise in MRI*, pages 31–71. Springer, 2016.
2. A. Buades, B. Coll, and J. M. Morel. A review of image denoising algorithms, with a new one. *Multiscale Model SIAM.*
3. G. Chen, Y.f. Wu, D.G. Shen, and P.T. Yap. XQ-NLM: Denoising diffusion mri data via xq space non-local patch matching. In *MICCAI*, pages 587–595, 2016.
4. C. Cocosco. Brainweb : online interface to a 3D MRI simulated brain database. *Neuroimage*, 5:425, 1997.
5. P. Coupe, S. Yger, P.and Prima, P. Hellier, C. Kervrann, and C. Barillot. An optimized blockwise nonlocal means denoising filter for 3D magnetic resonance images. *IEEE T. Med Imaging*, 27(4):425–441, 2008.
6. H.Hu, B.Li, and Q.Liu. Removing mixture of gaussian and impulse noise by patch-based weighted means. *J Sci Comput*, 67(1):103–129, 2016.
7. C.H. Lin, J.S. Tsai, and C.T. Chiu. Switching bilateral filter with a texture/noise detector for universal noise removal. *IEEE Image Process*, 19(9):2307–2320, 2010.
8. M. Maggioni, V. Katkovnik, K. Egiazarian, and A. Foi. Nonlocal transform domain filter for volumetric data denoising and reconstruction. *IEEE T Image processing*, 22(1):119–133, 2013.
9. J. Manjón, P. Coupé, A. Buades, D.L. Collins, and M. Robles. New methods for MRI denoising based on sparseness and self-similarity. *Med Image Anal*, 16(1):18–27, 2012.
10. S. Patz. The rician distribution of noisy MRI data. *Magn Reson Med*, 34(6):910–4, 1995.
11. C. Tomasi and R. Manduchi. Bilateral filtering for gray and color images. In *ICCV*, pages 839–846, 1998.
12. N. Wiest-Daesslé, S. Prima, P. Coupé, S. P. Morrissey, and C. Barillot. Rician noise removal by non-local means filtering for low signal-to-noise ratio MRI: applications to DT-MRI. *MICCAI*, 11(2):171–179, 2008.